Multiple tissue-specific requirements for the BMP antagonist *Noggin* in development of the mammalian craniofacial skeleton

Maiko Matsui *, John Klingensmith **

Department of Cell Biology, Duke University Medical Center, Durham NC27710, USA

ABSTRACT

Proper morphogenesis is essential for both form and function of the mammalian craniofacial skeleton, which consists of more than twenty small cartilages and bones. Skeletal elements that support the oral cavity are derived from cranial neural crest cells (NCCs) that develop in the maxillary and mandibular buds of pharyngeal arch 1 (PA1). Bone Morphogenetic Protein (BMP) signaling has been implicated in most aspects of craniofacial skeletogenesis, including PA1 development. However, the roles of the BMP antagonist Noggin in formation of the craniofacial skeleton remain unclear, in part because of its multiple domains of expression during formative stages. Here we used a tissue-specific gene ablation approach to assess roles of *Noggin* (*Nog*) in two different tissue domains potentially relevant to mandibular and maxillary development. We found that the axial midline domain of *Nog* expression is critical to promote PA1 development in early stages, necessary for adequate outgrowth of the mandibular bud. Subsequently, *Nog* expression in NCCs regulates craniofacial cartilage and bone formation. Mice lacking *Nog* in NCCs have an enlarged mandible that results from increased cell proliferation in and around Meckel's cartilage. These mutants also show complete secondary cleft palate, most likely due to inhibition of posterior palatal shelf elevation by disrupted morphology of the developing skull base. Our findings demonstrate multiple roles of Noggin in different domains for craniofacial skeletogenesis, and suggest an indirect mechanism for secondary cleft palate in *Nog* mutants that may be relevant to human cleft palate as well.

© 2014 Published by Elsevier Inc.

Introduction

Among the most frequently occurring congenital defects in newborns are craniofacial deformities, such as cleft palate and micrognathia (Holder-Espinasse et al., 2001; Mossey PA, 2002). These malformations impact the quality of life due to functional difficulties as well as negative social responses (Pruzinsky, 1992). The causes of craniofacial deformities are diverse, including genetic and environmental factors. Yet the underlying genetic and cellular mechanisms behind the emergence of such deformities are not well understood.

Mammalian craniofacial skeletal elements consist of more than 20 small bones and cartilages, the size and shape of which are precisely determined during development (reviewed by Matsui and Klingensmith (2013)). Most of these skeletal elements are derived from neural crest cells (NCCs), an ectoderm-derived multipotent cell population that migrates ventrally from the closing dorsal neural folds. NCCs take distinct migratory pathways,

with some populating the pharyngeal arches. One such group of NCCs populates pharyngeal arch 1 (PA1), where it proliferates and differentiates to give rise to most of the frontal facial skeletal structures, such as Meckel's cartilage, the mandible and the maxilla, including the bones of the palate. Although NCCs possess intrinsic information that promotes differentiation of the facial skeleton, interactions between NCCs and other tissues such as ectoderm or endoderm allow molecular signaling between tissues to ensure proper morphogenesis and development of pharyngeal arch derivatives (Couly et al., 2002).

Bone morphogenetic protein (BMP) signaling has been implicated as a key regulator of development of NCCs and their derivatives (Baek et al., 2011; Bonilla-Claudio et al., 2012; Dudas et al., 2004; Goldstein et al., 2005; Kanzler et al., 2000). Mouse genetic manipulation studies have revealed a requirement for precise regulation of BMP signaling in craniofacial development (Bonilla-Claudio et al., 2012; Li et al., 2013; Wang et al., 2013).

A critical means of regulating BMP signaling is by extracellular BMP antagonists. Noggin is a major BMP antagonist expressed in multiple domains during embryonic development. Noggin binds to BMP ligands in the extracellular space and prevents them from binding their receptors. Experimental work in mice indicates that Noggin regulates various types of skeletogenesis, including appendicular bone,

* Corresponding author.
** Corresponding author.
E-mail addresses: maiko.matsui@gmail.com (M. Matsui),
john.klingensmith@duke.edu (J. Klingensmith).

cartilage and joint formation (Brunet et al., 1998). Genetic studies in humans have also identified a role for the *NOGGIN* gene in regulating skeletal morphogenesis, with mild ectopic bone formation particularly in the digits, associated with heterozygous loss-of-function mutations (reviewed by Potti et al. (2011)).

As demonstrated primarily by analysis of the null phenotypes of mice lacking the *Noggin* (*Nog*) gene, this BMP antagonist also has important roles in regulating the development of craniofacial structures. For example, in postnatal stages of development, *Nog* expression in cranial sutures prevents the premature fusion of skull bones (craniosynostosis) (Warren et al., 2003). *Nog* null mice display cleft palate, a defect ascribed to compromised integrity of palatal epithelium due to the change in cell death and cell proliferation rate (He et al., 2010). Further essential roles of Noggin are revealed in the absence of Chordin (Anderson et al., 2002; Stottmann et al., 2001), another BMP antagonist which when lacking on its own has only very mild, non-lethal phenotypes (Choi and Klingensmith, 2009). These *Chrd;Nog* double mutant defects sometimes include dramatic truncations of the rostral head, in association with holoprosencephaly (Anderson et al., 2002; Bachiller et al., 2000). Such rostral defects are due at least in part to defective Shh signaling from the prechordal plate and Fgf8 signaling from the anterior neural ridge, organizing centers of early forebrain patterning and growth (Anderson et al., 2002).

Independent of this early rostral requirement, these BMP antagonists also function to promote mandibular development. Whereas mice lacking the *Chordin* gene (*Chrd*) show a very low penetrance of mild micrognathia (Choi and Klingensmith, 2009), $Chrd^{-/-};Nog^{+/-}$ and $Chrd^{-/-};Nog^{-/-}$ exhibit a spectrum of mandibular hypoplasia, ranging from agnathia to micrognathia, as a result of insufficient NCC survival during mandibular bud outgrowth (Stottmann et al., 2001). In contrast, in the absence of *Nog* alone, mandibles are enlarged, reflecting increased size of the transient Meckel's cartilage, around which mandibular bone is formed (Stottmann et al., 2001; Wang et al., 2013). The mandible forms via ossification of cells from the NCC-derived perichondrium at the periphery of Meckel's cartilage, which itself is composed of both neural crest derivatives and other mesenchymal cells (Chai et al., 2000a). Whereas the normal fate of chondrocytes in the main portion of Meckel's cartilage is to degenerate, in *Nog* mutants or in embryos expressing an activated BMP receptor transgene in chondrocytes, these cells over-proliferate, then differentiate and undergo ossification (Wang et al., 2013).

These phenotypes all reveal important roles for Noggin in regulating development of the craniofacial skeleton, but the relevant spatiotemporal contexts of *Nog* expression are not clear for any of these roles. During early stages of head development, *Nog* is expressed in several potentially relevant domains (Anderson et al., 2002; He et al., 2010; Lana-Elola et al., 2011; Nifuji and Noda, 1999; Stottmann et al., 2001). Here we further probe the expression of *Nog* in relation to development of the viscerocranium. We then use a series of tissue-specific ablations of the *Nog* gene to elucidate the cellular mechanisms of Noggin function in mandibular and palatal development.

Results

Expression of Nog during formative craniofacial development

To gain insight into the possible roles of Noggin in development of tissues derived from PA1, we assessed its spatiotemporal expression using an assay for expression of a *lacZ* reporter integrated into the published *Nog* null allele (Anderson et al., 2002; Brunet et al., 1998; McMahon et al., 1998). *Nog* is expressed transiently in migrating and postmigratory NCCs from the earliest

stages, with robust expression by at E8.5 (Fig. 1(A) and (B)). At E9.5 expression is observed in NCCs in PA1 (Fig. 1(C) and (E)). By E10.5, its expression is greatly diminished in the PA1 mesenchyme and is largely restricted to the arch ectoderm (Fig. 1(D) and (F)). Over this timeframe *Nog* is also present in the notochord, the floor plate of the neural tube, the dorsal foregut endoderm (Fig. 1(B) and (C)), as well as the ventrolateral foregut endoderm in the laryngeal region. Later, during palatal development at E11.5 and E13.5, *Nog* is strongly expressed in the palatal epithelium (Fig. 1(G) and (H)). *Nog* is also expressed in various cartilages; as previously observed (Wang et al., 2013), this includes Meckel's cartilage from E12.5 and later (Fig. 1G,H).

Loss of BMP antagonism specifically from axial domains results in mandibular truncations but not cleft palate

The early onset and forebrain gene expression changes in *Chrd; Nog* double mutants indicate that the axial midline expression of these BMP antagonists is key for forebrain development (Anderson et al., 2002). Given that in the absence of *Chrd*, loss of one or both wildtype alleles of *Nog* can also result in mandibular hypoplasia, independent of holoprosencephaly phenotypes (Anderson et al., 2002; Stottmann et al., 2001), we sought to determine whether the outgrowth defect also reflected loss of the axial domain of *Nog*, or another early domain such as cranial NCCs. We tested the role of axial *Nog* in craniofacial development by deleting *Nog* in the axial midline from early stages, with or without the presence of a wildtype *Chrd* allele. To remove *Nog* function exclusively from the axial midline, we combined a conditional null allele of *Nog* (Nog^{fx}) (Stafford et al., 2011) with *Shh-GFP-Cre* (Harfe et al., 2004), a recombination driver for the late node, notochord, and floor plate. Because these are all sites of both *Nog* and *Chrd* expression, we generated *Shh-GFP-Cre*;$Nog^{lacz/fx}$ mutants with and without the presence of *Chrd*. As expected from previous studies (Stottmann et al., 2001; Anderson et al., 2002), we did not see holoprosencephaly or mandibular arch phenotypes in the *Shh-GFP-Cre*; $Nog^{lacz/fx}$ mutants in the presence of wildtype *Chrd* (data not shown). In contrast, *Shh-GFP-Cre*; $Nog^{lacz/fx}$; $Chrd^{-/-}$ embryos displayed partially penetrant hypoplastic PA1 phenotypes, including diminished mandibular and maxillary structures (3/5); some of these mutants were holoprosencephalic as well (Fig. 2(A)–(D)). These data collectively indicate that the rostral truncation phenotypes of *Chrd;Nog* mutants, including both forebrain and mandibular arch truncations, result from a deficit of axial midline BMP antagonism by Chordin and Noggin. Thus, Noggin function in axial midline tissues promotes mandibular outgrowth, though none of these tissues contribute to the mandible.

None of the embryos lacking *Nog* specifically in the axial midline (*Shh-GFP-Cre*; $Nog^{lacz/fx}$;$Chrd^{-/-}$) showed two relevant defects of the *Nog* null: None exhibited a thickening of the mandible (Fig. 2(G) and (H)), implying that some other deficit of *Nog* underlies the thickened mandible phenotype of the null (Stottmann et al., 2001; Wang et al., 2013). Furthermore, the embryos lacking axial *Nog* did not display cleft palate. This indicates that the fully-penetrant cleft palate defect of *Nog* null mutants (He et al., 2010) does not result from a lack of axial BMP antagonism, but instead implies another tissue type must make Noggin protein for proper development of craniofacial structures, including palatogenesis.

Loss of Nog in neural crest cells results in an enlarged mandible

Since many craniofacial skeletal elements are derived from NCCs, in which *Nog* is expressed (Stottmann et al., 2001), we assessed potential roles of *Nog* in NCCs using *Wnt1-Cre*, an NCC specific Cre driver (Danielian et al., 1998), in the development of
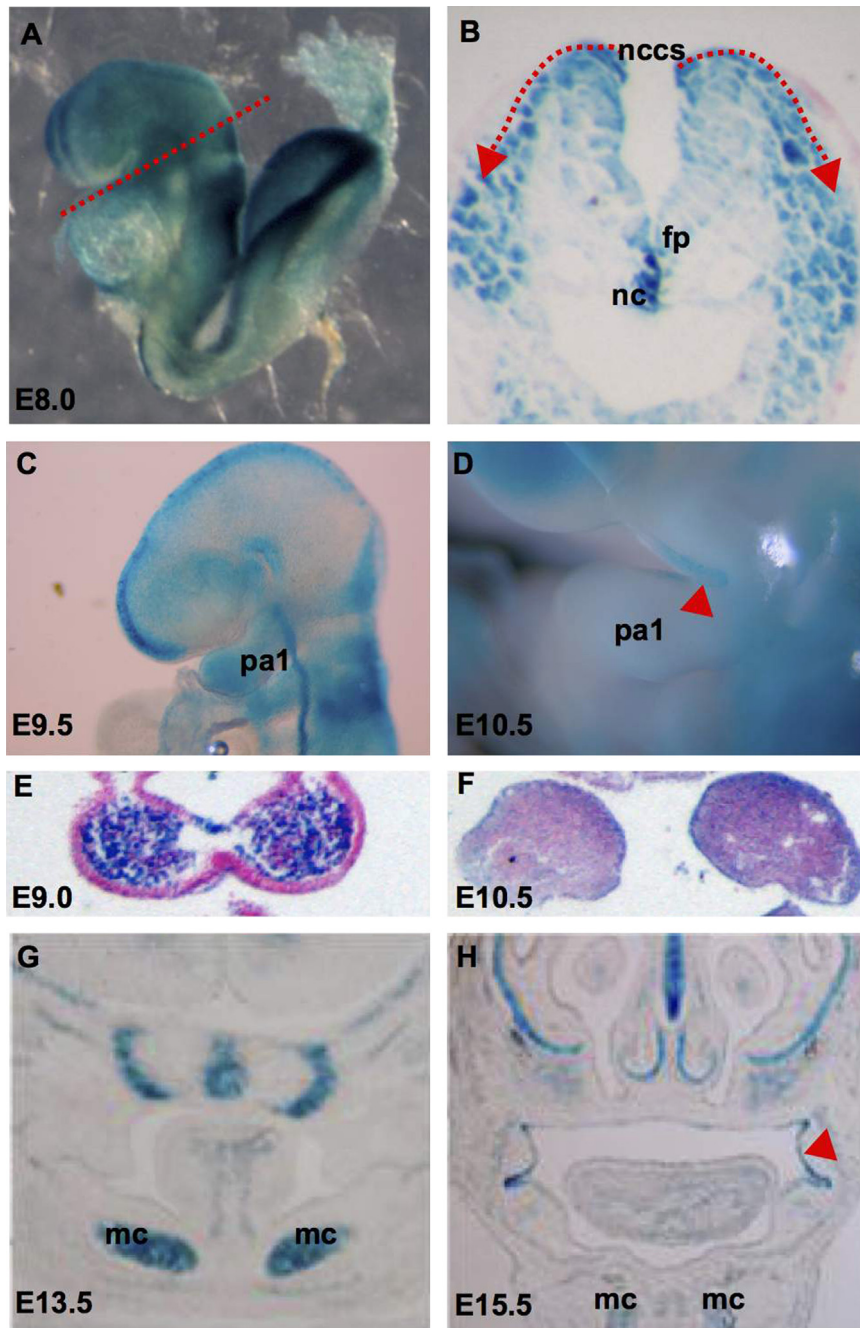
Fig. 1. *Nog* is expressed in multiple domains during craniofacial development. (A) and (B) *Nog* is first expressed in migrating NCCs around E8.0. (C) *Nog* is expressed in the NCCs of PA1. (D) By E10.5 *Nog* expression is restricted to the oral epithelium of PA1. (E) and (F) Sections through PA1 showing transient expression of *Nog*. At E9.0, *Nog* expression is found in mesenchyme of PA1 (E), but *Nog* expression subsequently shifts to the epithelium layer of PA1 (F). (G) and (H) *Nog* is expressed in the cartilages of the head. pa1; pharyngeal arch 1, fp; floor plate of the neural tube, mc; Meckel's cartilage, nccs; neural crest cells, ns; nasal septum, oe; oral epithelium.

craniofacial structures. In the head region, *Wnt1-Cre* is expressed in the dorsal neural folds from early stages of cranial NCC development, as well as in newly migrating NCCs (Jiang et al., 2000; Stottmann and Klingensmith, 2011). Given that *Chrd* is redundant with *Nog* in many developmental contexts (reviewed by (Klingensmith et al., 2010), and that PCR data suggest *Chrd* is expressed at low levels in NCCs (M. Choi and JK, unpublished results), we tested the role of *Nog* in NCCs with and without wildtype allele(s) of *Chrd*. We found that the craniofacial phenotypes of *Wnt1-Cre; Nog^{lacz/fx}* animals were not noticeably different from *Wnt1-Cre;Nog^{lacz/fx};Chrd^{−/−}* (Supplementary Fig. 1). Regardless of *Chrd*'s presence or absence, embryos lacking *Nog* from NCCs displayed very similar if not identical craniofacial defects. As a

demonstration, the samples in Fig. 3 are from mutant animals of the genotype *Wnt1-Cre; Nog^{lacz/fx};Chrd^{−/−}*, whereas all other figures depict results from mutants that were *Wnt1-Cre; Nog^{lacz/fx}*.

A striking phenotype in embryos lacking *Nog* in NCCs is an enlarged mandible (Figs. 3 and 4(A) and (B)), very similar to that of *Nog* null mice (Stottmann et al., 2001; Wang et al., 2013). Other craniofacial skeletal derivatives of NCCs, including laryngeal structures such as the hyoid and thyroid cartilages, were also hypermorphic in the mutant embryos (Supplementary Fig. 2). Our results indicate that the thickened mandible phenotype of *Nog* mutants is due specifically to a lack of Noggin in NCCs, implying that attenuation of BMP signaling in the immediate environment of NCCs is necessary for proper mandibular morphogenesis.
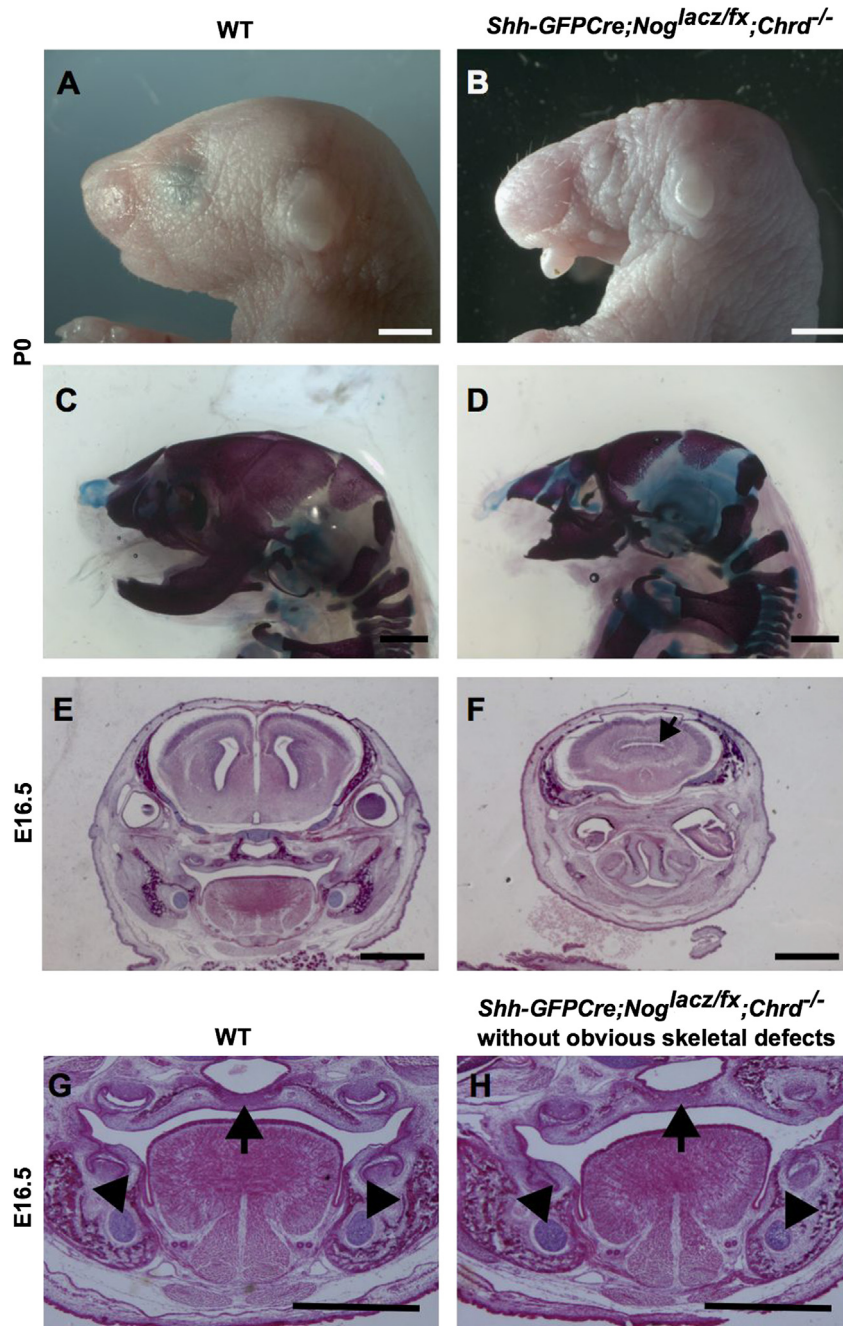
WT   *Shh-GFPCre;Nog^{lacz/fx};Chrd^{-/-}*

Fig. 2. BMP antagonism in axial domain is critical for development of PA1 derivatives. (A)–(D) Lateral view of wild-type (A) and (C) and *Shh-GFPCre;Nog^{lacz/fx};Chrd^{-/-}* (B) and (D) mutant whole-mount and skeletal-preparation heads at P0 stage showing that a lack of *Chrd* and *Nog* in the *Shh-GFPCre* domain results in hypomorphic PA1 derivatives compared with wild-type littermates. Scale bars=2 mm. (E) and (F) Example of holoprosencephaly in mutant embryo at E16.5 (F), and with a normal littermate (E). (G), and (H) Mutant embryos without obvious phenotypes showing relatively normal development of the palate (indicated with an arrow) and Meckel's cartilage (indicated with arrowheads (H)). Scale bars=1 mm.

Neural crest migration into PA1 occurs normally in embryos lacking Nog in NCCs

We investigated the mechanisms underlying the enlarged mandibular skeletal element. A potentially relevant finding is that BMP signaling promotes delamination and collective migration of NCCs (Burstyn-Cohen and Kalcheim, 2002; Hall and Erickson, 2003). In so far as *Chrd^{-/-};Nog^{+/-}* embryos have increased neural crest production from the neural tube (Anderson et al., 2006), we hypothesized that ablating *Nog* from NCCs might increase production and migration of NCCs into the pharyngeal arches. However, we observed that the size of the PA1 in mutant embryos was not noticeably larger than that in wild type littermates at E10.5, when NCC migration is completed (Supplementary Fig. 3). We also assessed the expression of pharyngeal arch markers, including *Dlx2, Dlx5, Msx1*, and *Barx1* (Supplementary Fig. 3). We detected no altered expression relative to wild type embryos, suggesting normal early patterning of the arch mesenchyme and ectoderm. These results suggest that altered NCC production and emigration into PA1 are not the primary cause of the enlarged mandibular skeleton observed in *Wnt1-Cre;Nog^{lacz/fx}* mutants.
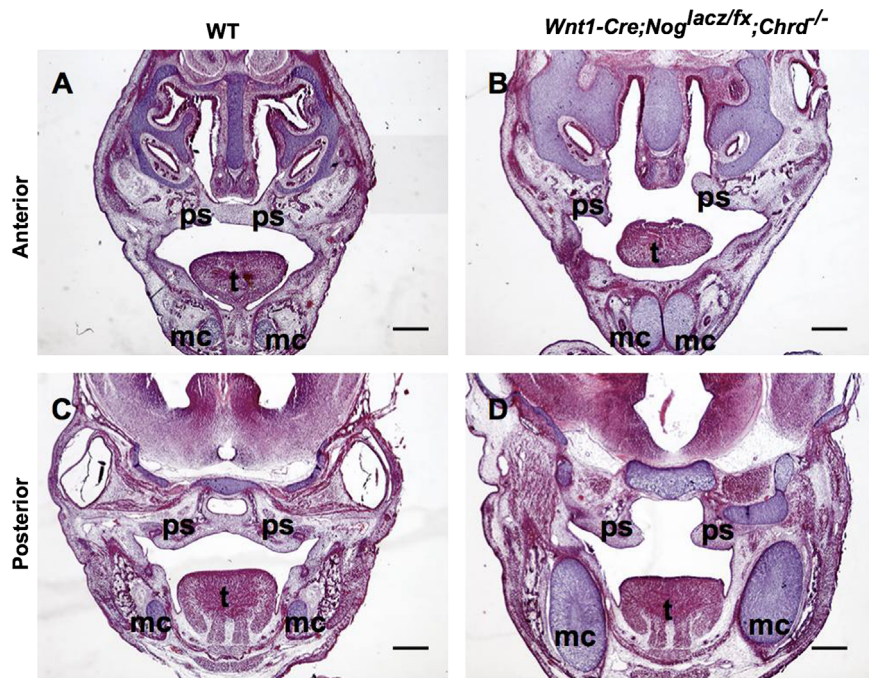
Fig. 3. Absence of *Nog* in NCCs causes craniofacial defects. (A) and (C) Anterior and posterior coronal sections through E15.5 wild-type embryonic head showing fusion of the palatal shelves and normal development of cartilages in the head. (B) and (D) Anterior and posterior coronal sections of *Wnt1-Cre;Nog^{lacz/fx};Chrd^{−/−}* mutant embryos showing cleft palate and enlarged cartilages at E15.5. ps; palatal shelves, t; tongue, mc; Meckel's cartilage. Scale bars=400 μm.

Cell proliferation in Meckel's cartilage and perichondrium is increased in the absence of Nog in neural crest derivatives

To probe the cause of the enlarged mandible in mutants lacking *Nog* in NCCs, we performed cell proliferation assays in Meckel's cartilage using a BrdU incorporation and detection assay to mark proliferating cells. Meckel's cartilage first forms as a cartilage condensation around E11.5. At this stage, there is little difference in the size of the condensation between wild type and mutant embryos (Fig. 4(C) and (D)). However, by E12.5, Meckel's cartilage begins to grow faster and larger in mutants relative to wild type littermates. Cell proliferation is increased at E12.5 both in the mesenchyme and in the perichondrium of mutant Meckel's cartilage, and the diameter of Meckel's cartilage grows continuously larger in the mutant than in wild type until E15.5 (Fig. 4(E), (F), (J) and (K)).

Previous studies suggest that Hh signaling may regulate cell proliferation during mandibular development. For example, lack of Hh signaling in NCCs results in a hypoplastic mandible (Jeong et al., 2004; Melnick et al., 2005), whereas activating Hh signaling in NCCs increases the size of facial primordial (Jeong et al., 2004). Accordingly, one hypothesis for the increased mandibular size and cell proliferation in embryos lacking *Nog* in NCCs is upregulation of Hh signaling when BMP receptor activation is increased in NCCs due to a loss of *Nog* from these cells.

To investigate if activating BMP signaling in NCCs induces ectopic Hh signaling in the developing mandible, we assessed the state of Hh signaling upon forced elevation of BMP signaling in NCCs. To do this, we drove expression of an activated BMP receptor 1A (*caBMPr1a*) transgene (Rodriguez et al., 2010) specifically in NCCs, and included a *Ptch1-lacz* transgene, an established, obligate reporter of Hh signaling (Goodrich et al., 1997). At E13.5, Ptch1-lacz staining was apparent in the Meckel's cartilage of these *Wnt1-Cre*; *caBMPr1a*; *Ptch1-lacz* mutants, while no blue cells were found in the wild-type Meckel's cartilage (Fig. 4(G) and (H)). We also performed quantitative real time PCR (qPCR) to assess the level of Hh signaling and to determine if the increased Hh signaling

activity might be reflected by increased expression of any Hh ligand. Our qPCR results showed increased expression of Hh transcriptional target genes at E12.5 (Fig. 4(L)). Moreover, we observed that *Indian hedgehog* (*Ihh*) expression is significantly increased in the mutant mandible. Together, these data suggest that in mandibular NCCs, increased BMP receptor activation leads to increased *Ihh* transcription, which then leads to increased Hh signaling, a putative NCC mitogen. This in turn implies that the enlarged mandibular phenotype of embryos lacking *Nog* in NCCs may result from increased cell proliferation caused by elevated Hh signaling.

Absence of Noggin in NCCs results in secondary cleft palate

Beyond an enlarged mandible, loss of *Nog* expression in NCCs also results in other craniofacial skeletal defects. While many defective skeletal elements are enlarged in mutants, such as the nasal cartilage, hypoplasia occurs in a few membranous bones, such as the palatal bone (Fig. 8(J) and (K)) and those of the cranial vault (data not shown). Although primary palatal development appeared unaffected in embryos lacking *Nog* specifically in neural crest derivatives, *Wnt1-Cre*;*Nog^{lacz/fx}* embryos show overt secondary cleft palate (Fig. 5). Although the cause of cleft palate in *Nog* mutants was previously attributed to a lack of *Nog* expression in the oral epithelium (He et al., 2010), our results indicate that a key contributor to the cleft palate phenotype in *Nog* nulls is a lack of *Nog* in NCCs.

To investigate the etiology of the palatal defects in *Wnt1-Cre; Nog^{lacz/fx}* mutant mice, we performed detailed morphological and histological analyses of palatal shelves at different stages of development. We first assessed the growth of the palatal shelves. At E13.5 palatal shelves of control and mutant embryos showed no clear differences in shape or size (Fig. 6(A) and (F)). We used a BrdU incorporation assay to assess cell proliferation in the palatal shelf mesenchyme at this stage. We saw no significant difference between wild type and mutant embryos (Fig. 6(M) and (N)). Thus both the gross size and shape of the palatal shelves, as well as cell
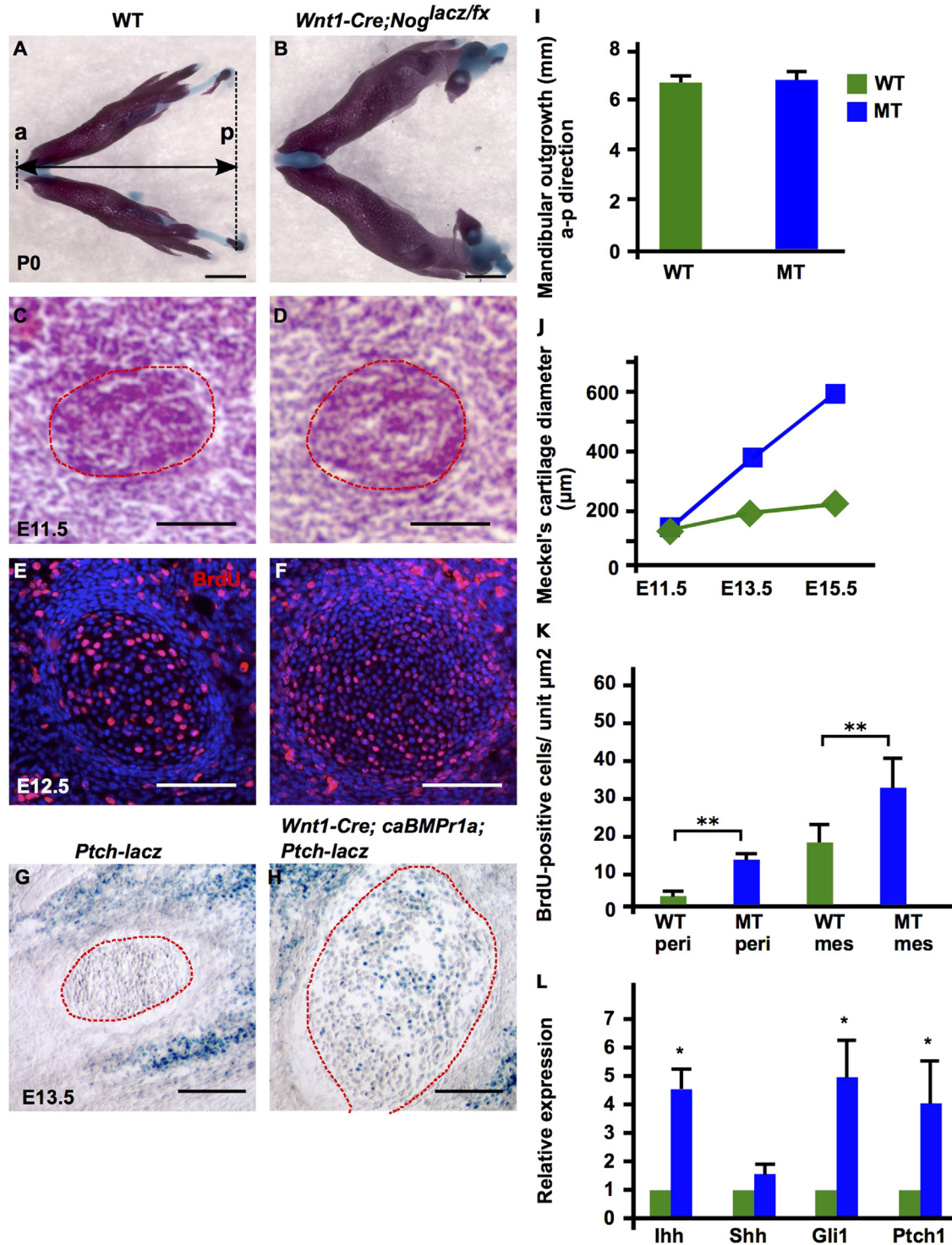
Fig. 4. An enlarged Meckel's cartilage with increased cell proliferation results from upregulation of BMP signaling in neural crest derivatives. (A) and (B) Mandibular skeletal preparations. Wild type mandible (A) shows normal development of Meckel's cartilage (blue) and mandibular bone (purple). Double headed arrow shows antero–posterior (a-p) direction of mandibular outgrowth. Enlarged Meckel's cartilage in *Wnt1-Cre;Nog^{lacz/fx}* mutant (B) shows no obvious outgrowth defects. Scale bar=1 mm. (C) and (D) Meckel's cartilage surrounded by a red dotted line. The size of wild type (C) Meckel's cartilage is similar to mutant (D) at E11.5. Scale bars=100 μm. (E) and (F) Cell proliferation in Meckel's cartilage as indicated by BrdU incorporation. Compared with cell proliferation in wild-type Meckel's cartilage (E), cell proliferation was increased in the mutant Meckel's cartilage at E12.5 (F). Scale bars=100 μm. (G) and (H) Meckel's cartilage surrounded by a red dotted line. Expression of a constitutively active BMP receptor 1a (*caBMPr1a*) in combination with *Wnt1-Cre* caused ectopic expression of Hh signaling in mutant Meckel's cartilage, as revealed by blue staining of Ptch-lacz activity at E13.5 (H). Wild-type (G) Meckel's cartilage showed no beta-galactosidase activity. Scale bar=100 μm. (I) Mandibular outgrowth in the antero–posterior direction as shown in (A) is not different between wild-type and mutant embryos. (J) The diameter of Meckel's cartilage showed similar size between wild-type and mutant at E11.5. However, after E12.5 mutant Meckel's cartilage started rapidly growing and the growth persisted at E15.5, while growth rate in wild-type Meckel's cartilage was diminished. (K) Increased cell proliferation in both perichondrium (peri) and mesenchyme (mes) in Meckel's cartilage of *Wnt1-Cre;Nog^{lacz/fx}* mutant was statistically significant at E12.5. (L) qPCR indicates increased expression of Hh signaling targets (Gli1, Ptch1) and the Ihh ligand gene in the mutant Meckel's cartilage at E12.5. $P < 0.05$.
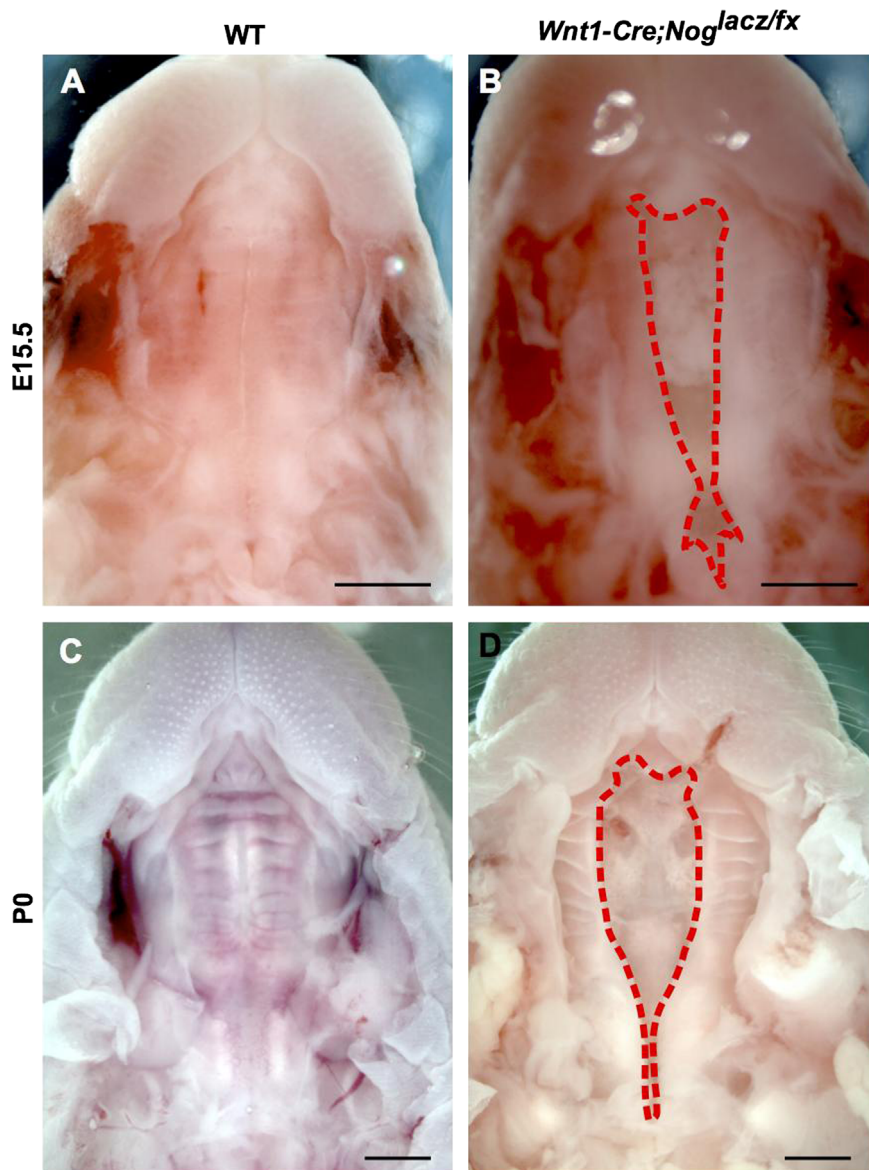
Fig. 5. *Nog* in NCCs is required for proper palatogenesis. (A) and (B) Ventral views of palatal structure. A wild-type E15.5 mouse (A) showing normal palatal development in which the palatal shelves have fused by this stage, compared with the secondary cleft palate in a *Wnt1-Cre;Nog^lacz/fx* embryo (B). (C) and (D) Ventral views of palatal structure in newborn pups (P0). A wild-type P0 mouse showing normal palatal development (C). Overt cleft palate in *Wnt1-Cre;Nog^lacz/fx* is obvious at P0 (D). Scale bars=1 mm.

proliferation within the largely NCC-derived mesenchyme, show no difference.

We next tested whether patterning markers are correctly expressed in the mutant palatal shelves. During palatal development, specific genes are expressed along the anterior–posterior axis of the secondary palatal shelves. These gene expression patterns are informative markers to assess patterning defects in the mutant palatal shelves. *Shox2* is normally expressed in the anterior palatal shelves (Yu et al., 2005). *Shox2* null mice exhibit a rare form of cleft palate in which primary and secondary palatal shelves do not fuse properly (Yu et al., 2005). *Shox2* expression is greatly reduced in the anterior palatal shelves of *Nog* null embryos at E13.5 (He et al., 2010). By contrast, *Shox2* expression was not altered in the palatal shelves of *Wnt1-Cre;Nog^lacz/fx* embryos (Fig. 7 (A) and (E)). This indicates that it is not the NCC domain of *Nog* that regulates *Shox2* expression, though *Nog* appears to do so in some other palatal context.

Besides being a patterning marker for the developing palate, *Tbx22* is also a context-dependent downstream target gene of BMP signaling (Higashihori et al., 2010). Explant culture experiments

using facial primordia and palatal shelves suggest that *Tbx22* expression is regulated by BMP signaling (Fuchs et al., 2010). Its expression in the palatal shelves occurs posteriorly. Loss of *Tbx22* results in submucous cleft palate in mice and human (Braybrook et al., 2001). *Tbx22* null mice show reduced palatal bone due to delay in the osteoblast maturation (Pauws et al., 2009). However, in situ hybridization results showed that *Tbx22* expression is not altered in the *Wnt1-Cre;Nog^lacz/fx* mutant palatal shelves at E13.5. qPCR analysis also indicates that expression level of *Tbx22* is unchanged in the mutant palatal shelves relative to wild type tissue (Supplementary Fig. 4), although the eventual size of the palatal bone is greatly reduced (Figs. 7(B) and (F), and 8(J) and (K)). These results, as well as the lack of evidence for a change in cell proliferation in the mutant palatal shelves suggest that altered *Tbx22* expression in the *Wnt1-Cre;Nog^lacz/fx* palatal shelves is not the main cause of the smaller palatal bone and cleft palate in this mutant. Two other palatal shelf markers, *Barx1* and *Efnb2*, are also similarly expressed between wild-type and mutant embryos (Fig. 7 (C), (D), (G), and (H)). Collectively, our results with gene expression markers of palatal pattern formation suggest that patterning
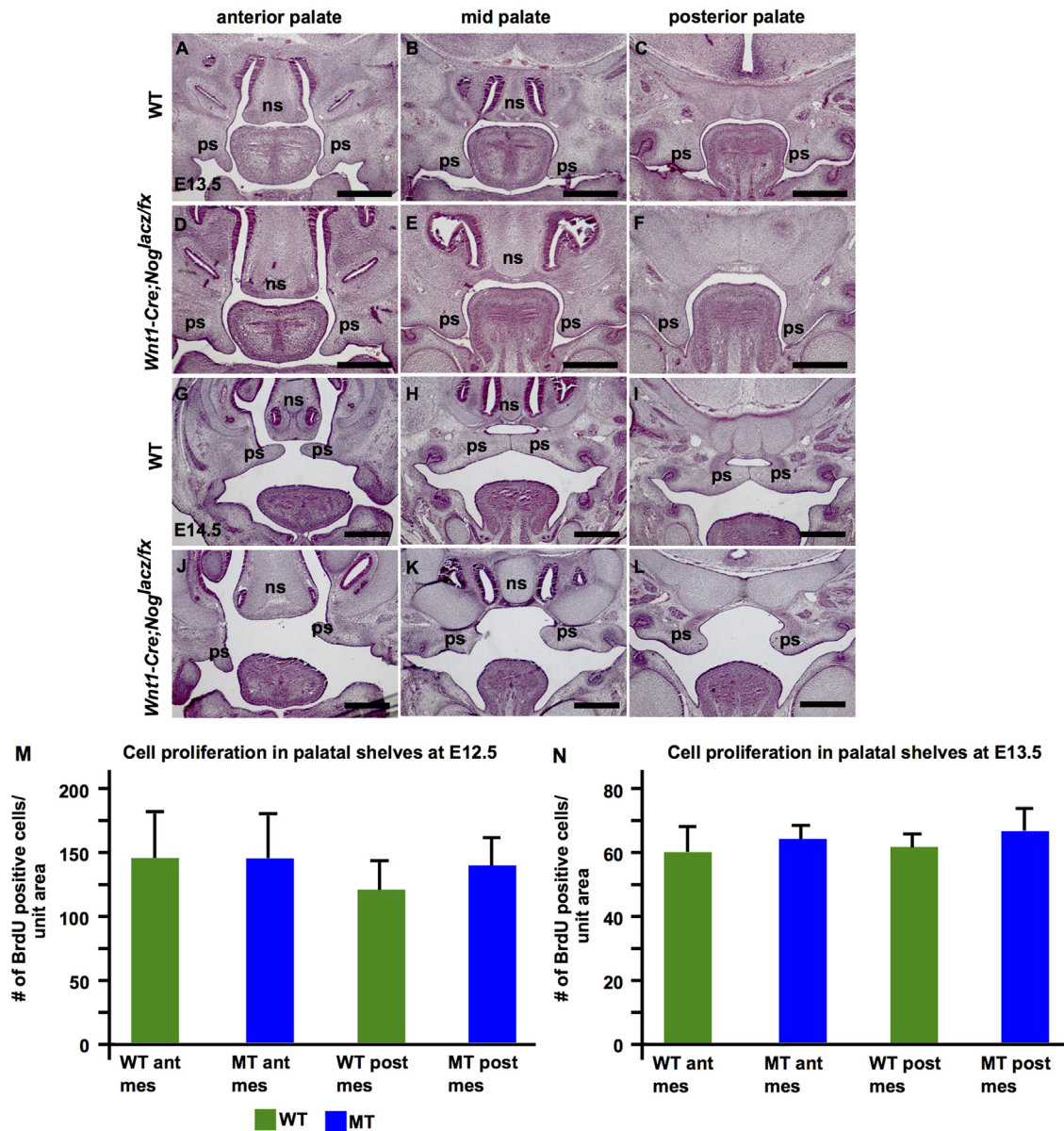
Fig. 6. Palatal shelf development in *Wnt1-Cre;Nog^{lacz/fx}* appears normal before elevation. (A)–(F) Anterior to posterior level matched coronal sections of E13.5 control (A)–(C) and mutant (D)–(F) littermates. (G)–(L) Anterior to posterior level matched coronal sections of E14.5 control (G)–(I) and mutant (J)–(L) littermates. Sections shown in the left column (A) and (D) are anterior secondary palate. Sections shown in the left column (G) and (J) are from the elevated secondary palate region. Mutant palatal shelves (J) often show incomplete elevation of palatal shelves. Sections shown in the middle column (B), (E), (H) and (K) are from the middle of the secondary palate region. Sections shown in the right column (C), (F), (I), and (L)) are from the posterior soft palate region. (M) and (N) numbers of BrdU-positive cells per unit area in the palatal shelves of E12.5 (M) and E13.5 (N) were counted and compared between wild-type and *Wnt1-Cre;Nog^{lacz/fx}* mutant littermates. They showed no statistically significant difference in cell proliferation. ns, nasal septum; ps, palatal shelf. Scale bars=400 μm.

failures are not a major cause of the cleft palate phenotype that occurs when Noggin is absent from neural crest derivatives.

Nog in NCCs is not required for palatal fusion

One of the common causes of cleft palate is a defect in palatal fusion. For the bilateral palatal shelves to properly fuse, the two sides need to be closely juxtaposed, with their binding aided by secretion of extracellular matrix (d'Amaro et al., 2012; Gato et al., 2002; Morris-Wiman and Brinkley, 1992). Upon contact of the opposing palatal shelves, dynamic tissue remodeling, including apoptosis and changes in gene expression, occur at the medial edge epithelium (MEE) (Huang et al., 2011; Nawshad et al., 2007; Xu et al., 2006). To test whether the neural crest domain of *Nog* is important for palatal fusion per se, we performed palatal

shelf explant cultures. Palatal shelves were harvested from E13.5 embryos, and then placed in contact with each other in culture medium such that their medial surfaces were juxtaposed. After 72 h, both wild-type and mutant palatal shelves fused normally (Fig. 7(I) and (J)). These data indicate that *Nog* expression in neural crest derivatives is not necessary for palatal fusion, in turn suggesting that failure of palatal shelf fusion is not the cause of the secondary cleft palate phenotype that occurs when Noggin is absent from NCCs.

Failed palatal shelf elevation likely results from dysmorphic skull base structure

As noted above, the size of the palatal shelves in *Wnt1-Cre; Nog^{lacz/fx}* mutant embryos prior to palatal shelf elevation showed
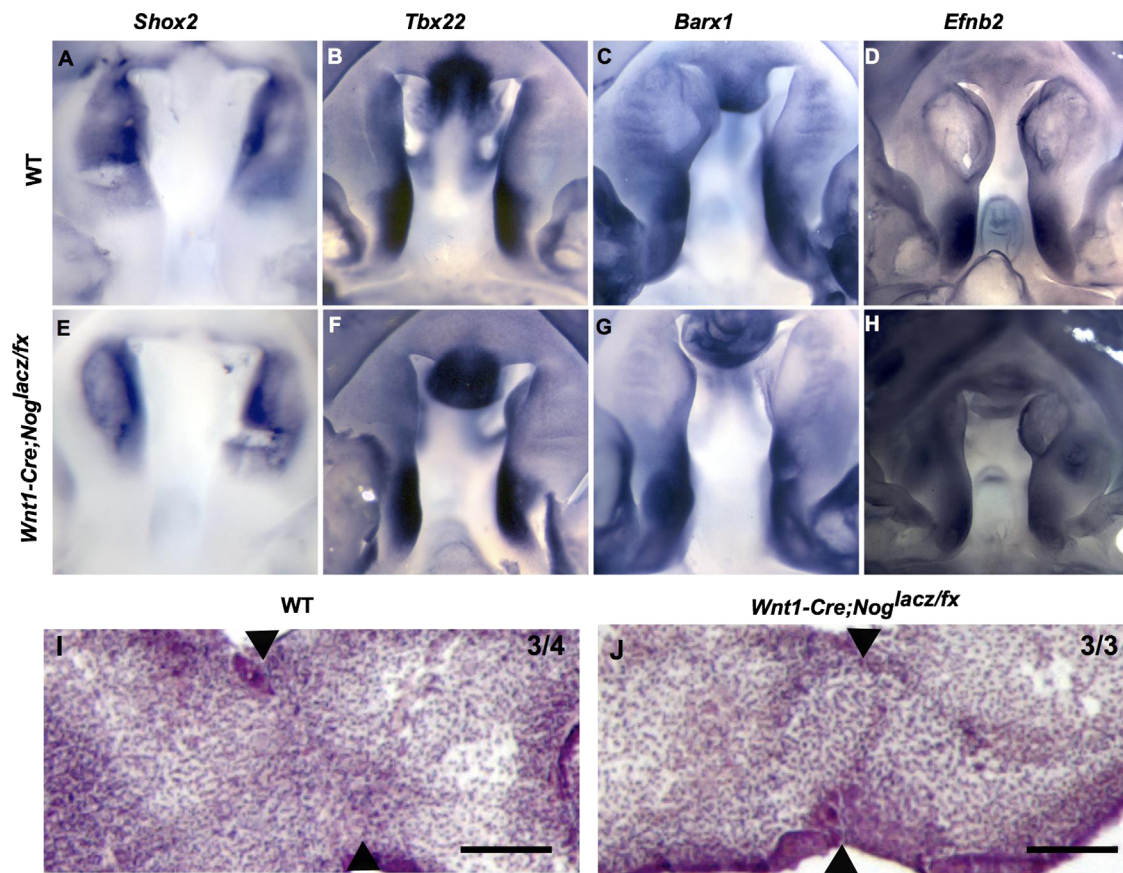
Fig. 7. Lack of *Nog* in NCCs does not prevent normal patterning or fusion steps of palatal development. (A)–(E) Anterior and posterior local patterning characteristics in the secondary palatal shelves are not altered in the *Wnt1-Cre;Nog$^{lacz/fx}$* mutant mice. (A) and (E) *Shox2* mRNA expression was restricted to the anterior palatal shelves in E13.5 wild-type (A) and mutant (E) littermates. (B)–(D, (F)–(H) Expression of *Tbx22* (B) and (F), *Barx1* (C) and (G), and *Efnb2* (D) and (H) mRNA was restricted to the posterior region of the E13.5 palatal shelves in both wild-type (B)–(D) and mutant (F)–(H) embryos. (I) and (J) Histological sections of cultured wildtype (I) and *Wnt1-Cre;Nog$^{lacz/fx}$* mutant (J) palatal shelves juxtaposed in culture show that both genotypes can fuse normally. Arrowheads indicate the point where palatal shelf fusion has taken place. Scale bars = 100 μm.

no overt differences relative to wild-type samples at E13.5. However, at E14.5 anterior palatal shelves were elevated horizontally above the tongue, yet were not close to each other; by contrast, control palatal shelves were fusing at this stage (Fig. 6 (G) and (L)). We observed that the angle of the mutant palatal shelves became wider progressively from anterior to posterior (Fig. 8(E) and (F)).

Upon analysis of sectioned samples, we observed ectopic skeletal element invasion into the posterior palatal shelves of mutant embryos at E13.5, at a stage in which palatal shelf elevation has not started (Fig. 8(A) and (B)). By E14.5, the ectopic skeletal tissue occupied much of the posterior palatal structure (Fig. 8(C) and (D)). Analysis of stained skeletal preparations revealed that the ectopic skeletal element in the posterior palatal shelves was an enlarged, dysmorphic pterygoid bone (Fig. 8 (H) and (K)). The pterygoid is a neural crest derivative (McBratney-Owen et al., 2008), and thus is the product of cells devoid of Noggin.

Beyond the pterygoid's direct disruption of palatal structure, we also observed that the antero–posterior (AP) and medial–lateral (ML) lengths of skull base structure were abnormal in mutants. The AP length of mutant skull base was significantly less while the ML width of mutant skull base was wider than those of wild-type embryos (Fig. 8(J)–(L)). We also found that the presphenoid and the basisphenoid bones in mutant embryos fused inappropriately (Fig. 8(J) and (K)). It seems probable that the shorter skull base caused by abnormally fused presphenoid and basisphenoid bones displaces an enlarged pterygoid bone

anteriorly, which in turn allows the enlarged pterygoid bone to invade into the posterior palatal shelves, preventing proper elevation of the palatal shelves in the mutant lacking *Nog* in NCCs. Similar phenotypes were observed in *Nog* null embryos (Supplementary Fig. 5).

Discussion

In this study, we used tissue specific gene knockout mouse models to probe the roles of two distinct domains of *Nog* in regulating craniofacial development. We found that the axial midline domain of BMP antagonism is critical for outgrowth of the mandibular bud of PA1, which swells with the immigration of NCC cells. Our data suggest an indirect effect of axial Noggin in promoting the survival of these NCCs. Later, in NCCs and their derivatives, *Nog* activity regulates development of mandibular and maxillary craniofacial skeletal elements that are derived from NCCs. By upregulating BMP signaling in NCCs, loss of Noggin caused Meckel's cartilage to become strikingly enlarged as a result of greatly increased cell proliferation; this was accompanied by increased Hh signaling, a possible mitogenic cue for some NCC derivatives. We also found that mutants lacking *Nog* in NCC derivatives show secondary cleft palate, likely due to defects in bones of the skull base, particularly an enlarged pterygoid. Together, these results reveal distinct roles of Noggin in axial domains for early PA1 development and in the NCC lineage for regulating later development of craniofacial skeletal elements.
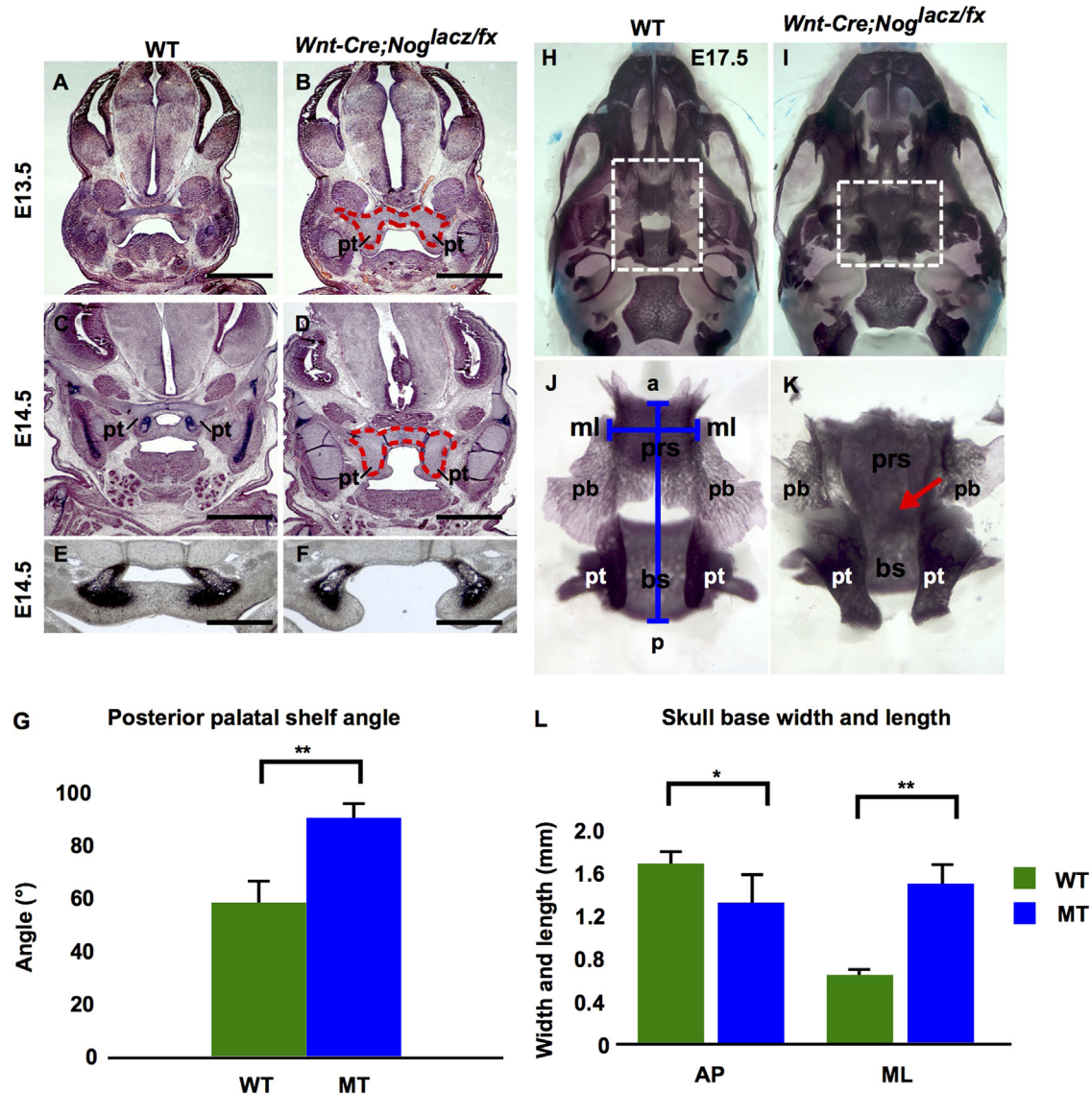
Fig. 8. Pterygoid bone disrupts the posterior palatal shelves in the *Wnt1-Cre;Nog^lacz/fx* mutant palate. (A)–(F) Coronal sections of heads from E13.5 and E14.5, comparing palatal structure in wild type and *Wnt1-Cre;Nog^lacz/fx* mutants. Before palatal shelf elevation at E13.5, the pterygoid bone is not obvious in this plane of section in the wild-type embryo (A), but it is already much larger in the mutant and invades into the posterior part of palatal shelves (B). (C) and (D) Coronal sections through posterior palate at E14.5. The pterygoid bone appears in wild-type at E14.5 (C), while it intrudes much further into mutant palatal shelves at this stage (D). (E) and (F) Coronal sections of palatal bone region at E14.5. Completely elevated and fused wild-type palatal shelves (E), whereas palatal shelves were elevated but the angle of elevation was wider in the *Wnt1-Cre;Nog^lacz/fx* mutant littermate (F). (G) The angle of palatal elevation was recorded and compared between wild-type and mutant littermates. (H) and (I) Skeletal preparation showing ventral view of the posterior skull base and the palate. Compared with the width of wild-type skull (H), the width of mutant skull is wider (I). (J) and (K) Isolated skull base and the palatal bone region from the skeletal preparations at E17.5. The bilateral palatal bones are in contact in wild-type embryo (J). In the mutant (K), the palatal bones are smaller and far apart, the pterygoid bone is enlarged and dysmorphic. (L) The length and width of the skull base were recorded and compared between wild-type and mutant skeletal preparations at E17.5. pb, palatal bone; pt, pterygoid bone; prs, presphenoid; bs, basisphenoid; a, anterior; p, posterior; ml, medial–lateral. *P-value < 0.05, **P-value < 0.01. Scale bars = 100 μm for (A), (B), (C), and (D), 500 μm for (E) and (F).

BMP antagonism by Noggin and Chordin from the axial midline promotes mandibular outgrowth

Our previous studies with *Chrd^−/−;Nog^−/−* and *Chrd^−/−;Nog^+/−* embryos revealed a requirement for the Chordin and Noggin BMP antagonists in proper generation of the NCCs that populate PA1 (Anderson et al., 2006; Stottmann et al., 2001). Lowering the genetic dosage of *Nog* in the absence of *Chrd* caused an increased emigration of NCCs from the dorsal neural folds, but instead of expanded mandibular buds, they were deficient; this was because a high level of NCC apoptosis in the pharyngeal region (Anderson et al., 2006). One possibility was that lack of expression of these

BMP antagonists in NCCs causes their death and the resulting mandibular hypoplasia. This is not the case, because we saw no outgrowth defect when we ablated *Nog* specifically in NCCs, regardless of whether *Chrd* was present or not. Instead, we found that in the absence of *Chrd*, ablating *Nog* from the axial midline (notochord and floor plate) results in mandibular hypoplasia very similar to that observed in *Chrd;Nog* mutants. If *Chrd* were present, loss of *Nog* from the axial midline had no such effect. The axial midline domain of *Nog* is therefore the relevant source of expression, in which it is redundant with *Chrd*.

Our results imply that decreased BMP antagonism at the axial midline leads to a failure to attenuate BMP signaling in the
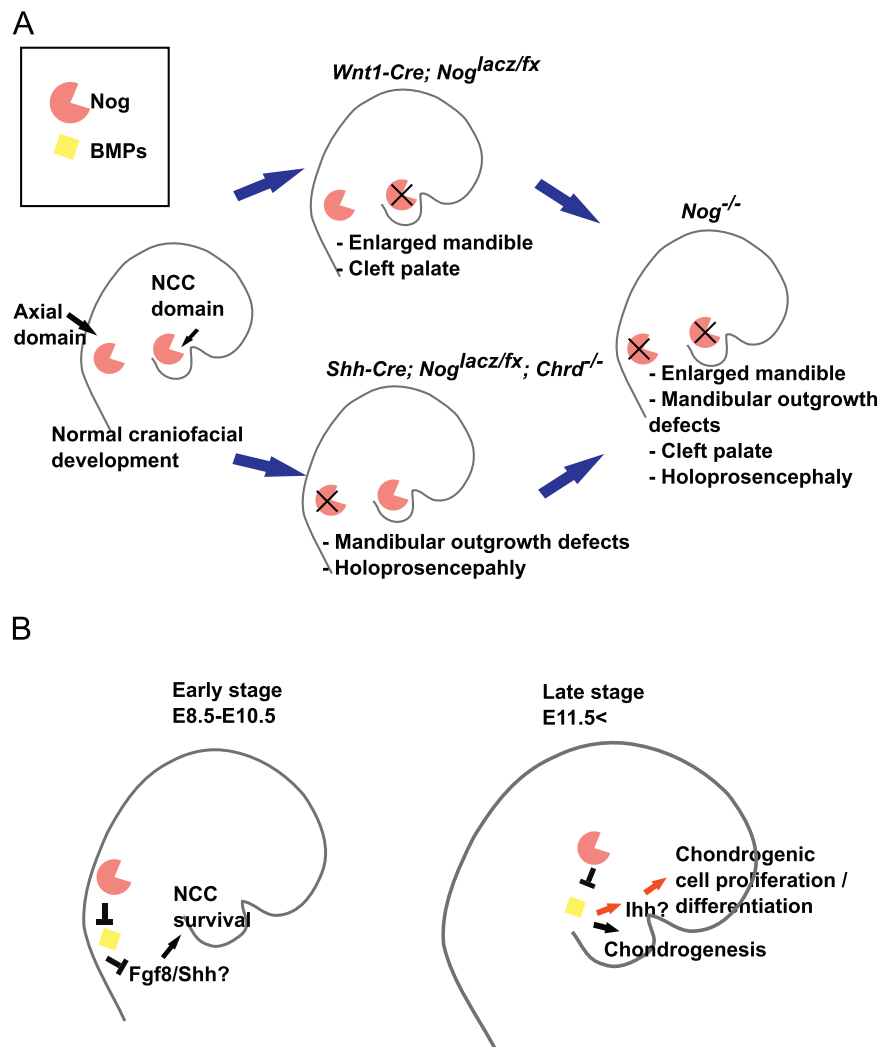
Fig. 9. Summary and model of the roles of *Nog* in development of craniofacial structures. (A) *Nog* is expressed in two relevant domains for craniofacial development—NCCs and axial midline. When *Nog* is ablated in NCCs, an enlarged mandible and cleft palate result without mandibular outgrowth defects. When the axial midline domain of *Nog* is absent, as well as *Chordin*, encoding a second midline BMP antagonist, mandibular outgrowth defects and holoprosencephaly occur. *Nog* null mutant embryos exhibit phenotypes of both of these tissue-specific mutants combined: enlarged mandible, cleft palate, mandibular outgrowth defects, and holoprosencephaly. (B) Earlier expression of *Nog* in axial domains promotes NCC survival by promoting secondary cues such as *Fgf8* and Hh signaling. However, at later stages, *Nog* regulates skeletogenesis by balancing the level of BMP signaling in and around NCC derivatives. In chondrocytes, *Nog* regulates the size of cartilage by suppressing cell proliferation. When BMP attenuation is insufficient, chondrocyte proliferation is promoted, possibly through ectopic *Ihh* expression and Hh pathway signaling.

pharyngeal environment as NCCs migrate through to populate the mandibular arch. One possibility is that increased BMP signaling in NCCs causes their apoptosis. If this were true, then expression of an activated BMP receptor in NCCs should cause their apoptosis. When we did this experiment, by expressing an activated BMP receptor (Rodriguez et al., 2010) in migratory NCCs, we saw the opposite phenotype—an enlarged mandible. Therefore, it is more likely that increased BMP activity caused by loss of axial BMP antagonism is leading to lower levels of an NCC survival cue. *Fgf8* has been shown to promote NCC survival during mandibular outgrowth. We previously found that pharyngeal *Fgf8* expression is reduced in *Chrd;Nog* mutants, and that beads soaked in BMP caused decreased expression of *Fgf8* in mandibular arch explants, whereas beads soaked in carrier had no effect (Stottmann et al., 2001). Together with these earlier results, our data further support a mechanism in which reduced axial BMP antagonism leads to increased pharyngeal BMP activity, which in turn reduces expression of *Fgf8* in the pharyngeal ectoderm and endoderm. This in turn results in less NCC survival as these cells colonize and populate the mandibular bud (Fig. 9).

Nog expression in NCCs regulates Meckel's cartilage and mandibular development

As noted above, loss of *Nog* expression from the NCCs, via tissue-specific gene ablation with *Wnt1-Cre*, resulted in an enlarged mandible. The enlarged mandibular phenotype is very similar to that seen in *Nog* nulls (Supplementary Fig. 5) (Stottmann et al., 2001; Wang et al., 2013). This phenotype was not noticeably different from *Wnt1-Cre;Nog^{lacz/fx};Chrd^{−/−}*, showing that loss of *Chrd* makes no difference when *Nog* is deleted specifically in the NCCs. In contrast, when the BMP antagonists Chordin and Noggin are both absent from the outset, mandibular bud outgrowth is deficient, and mandibular structures are greatly truncated. Thus in mandibular development per se, as opposed to mandibular bud outgrowth, there appears to be no redundancy of *Nog* with *Chrd*. Our results are consistent with a recent study which reported that BMP4 overexpression in NCCs at E12.5 resulted in a similar enlargement of Meckel's cartilage (Bonilla-Claudio et al., 2012). Earlier in development, embryos lacking *Nog* in NCCs (*Wnt1-Cre; Nog^{lacz/fx}* mice) showed normal size pharyngeal arches, and several

arch markers that are also BMP downstream target genes showed normal expression patterns at E10.5 (Supplementary Fig. 3). These results further suggest that *Nog* activity in NCCs is not necessary for early stages of mandibular development, but rather is necessary for proper skeletogenesis within the developing mandibular prominence.

We found that the enlarged mandible phenotype occurred not only when *Nog* was ablated from NCCs via *Wnt1-Cre*, but also when the same recombination driver was used to express an activated BMP receptor in NCCs. This result suggests that the NCCs themselves, and their derivatives, need attenuation of BMP signal transduction to undergo proper development in the mandibular bud. These derivatives are likely to be chondrocytes, as expression of an activated BMP receptor construct in these cells results in a similarly enlarged mandible as a result of expanded Meckel's cartilage (Wang et al., 2013).

Our studies with *Wnt1-Cre;Nog^{lacz/fx}* mutants indicated greatly increased cell proliferation in the perichondrial area of Meckel's cartilage relative to normal controls. A similar increase in cell proliferation was noted in embryos expressing an activated BMP receptor in chondrocytes (Wang et al., 2013). Consistent with studies suggesting the ability of BMP signaling upregulation in NCCs to cause increased cell proliferation in Meckel's cartilage (Hu et al., 2008; Wang et al., 2013), the increased size of the mandible may be a direct effect of an increased level of chondrocyte proliferation triggered by less attenuation of BMP signaling by Noggin. An alternative explanation is that the increased proliferation results form some other cue. We found that a known positive cytokine regulator of chondrocytic cell proliferation, *Indian hedgehog* (*Ihh*) (Minina et al., 2001), was expressed at increased levels when BMP signaling was upregulated in the NCC lineage. Accordingly, a second possibility is that in the context of the developing Meckel's cartilage, BMP signaling in NCCs positively regulates *Ihh* activity, which in turn promotes chondrocyte proliferation. At least in endochondral ossification, BMP signaling is reported to positively regulate *Ihh* expression which, in turn, promotes cell proliferation (Minina et al., 2002). This may be true in Meckel's cartilage as well. A caveat to this model is that in the absence of *Ihh*, in mutants lacking the gene, the size of the mandible is not greatly diminished (St-Jacques et al., 1999). We would thus posit that *Ihh* can promote chondrocyte proliferation in Meckel's cartilage, but is not essential for it. In any case, we suggest that a key function of Noggin in chondrocytes derived from NCC cells is to limit proliferation by attenuating BMP activity (Fig. 9).

Noggin activity and the regulation of palatal development

In addition to an enlarged mandible, *Wnt1-cre;Nog^{lacz/fx}* embryos exhibited almost fully penetrant secondary cleft palate. A previous study characterized the cleft palate of the *Nog* null (He et al., 2010), which also includes primary cleft palate. *Nog* is expressed in the oral epithelium, which showed increased cell death in *Nog* null mutants. He et al. (2010) expressed activated BMP receptor in the epithelium, and found that the resulting embryos had cleft palate. These findings suggested that the cleft palate of *Nog* mice results from increased BMP signaling in the oral epithelium. By contrast, we have found that ablation of *Nog* exclusively in the NCC lineage, which contributes to the mesenchyme but not the epithelium of the forming palate, also causes severe secondary cleft palate. Together, these studies suggest that *Nog* plays multiple tissue-specific roles in palatal development (Fig. 9(A)).

Palatal shelves from embryos lacking Noggin activity in NCC derivatives could fuse seemingly as well as in wild type in tissue culture experiments, but in the context of the rest of the mutant viscerocranium in vivo, they likely never get close enough. The mutant palatal bones were hypomorphic, which in principle could directly cause submucous cleft palate. However, the primary cause of overt cleft palate in *Wnt1-cre;Nog^{lacz/fx}* embryos seems more likely to be an indirect effect of defective viscerocranial skull formation which in turn disrupts posterior palatal morphogenesis. Palatal shelf elevation was likely inhibited by the presence of an enlarged pterygoid bone that is located posterior to the palatal shelves. The pterygoid precursor is derived from NCCs and develops through endochondral ossification (McBratney-Owen et al., 2008). These data suggest that a dysmorphic skull base element can greatly influence palatogenesis.

We further observed that in mouse fetuses lacking *Nog* in NCC derivatives, the skull base was shorter and wider than in wild type animals. Studies concerning human patients show great correlations between morphological anomalies in the skull base and the incidence of cleft palate. For example, in 3-month-old children with complete cleft, there was an increased width of the cranial base in newborns, compared with patients with incomplete cleft (Molsted et al., 1993; Molsted et al., 1995). Although a correlation between complete clefts and skull base anomalies was found, it is difficult to establish etiology from these results. Our mouse model suggests a mechanism of cleft palate in such cases: An abnormally formed bone outside those directly involved in palatal development can influence overall structural development of the skull base and indirectly cause cleft palate. It is likely that morphological anomalies in the skull base that affect palatal development are overlooked as part of the etiology of cleft palate.

Materials and methods

Mouse strains

The *Nog^{fx/fx}* conditional (Stafford et al., 2011), *Nog^{lacZ/+}* (Brunet et al., 1998), and constitutively active *Bmpr1a* conditional mice (*caBmpr1a*), conditional mice were maintained on a mixed background. *Wnt1-Cre* mice (Brewer et al., 2004; Chai et al., 2000b; Jeong et al., 2004; Jiang et al., 2000) were crossed with *Nog^{lacz/+}* to generate *Wnt1-Cre;Nog^{lacz/+}* male mice, which were subsequently crossed with *Nog^{fx/fx}* to conditionally knockout *Nog* from neural crest cells. As a complementary experiment, *caBmpr1a*, which have been described previously (Rodriguez et al., 2010), were crossed with *Wnt1-Cre* to activate BMP signaling in NCCs.

Histology, immunohistochemistry, and X-gal staining

For histology, embryos were harvested from pregnant mice, fixed in 4% paraformaldehyde (PFA) at 4 °C for 2 h to overnight depending on gestation stage, dehydrated through graded alcohols, embedded in paraffin wax and sectioned at 10-um thickness. The sections were stained with hematoxylin and eosin for histological observations.

Whole embryos were stained with X-gal overnight at room temperature (RT). For X-gal staining in sectioned material, embryos were fixed 2 h to overnight embedded in OCT compound (Sakura Finetek) after a sucrose gradient (15% and 30% sucrose in PBST). Cryosections were cut at 10 um thickness and stained with X-gal.

Skeletal preparations and in situ hybridization

For skeletal preparation, embryos were skinned, fixed in 95% ethanol overnight, stained with 0.05% alcian blue, washed in 95% ethanol for 6hours to overnight and cleared in 2% KOH. Further, to stain bone, embryos were placed in 0.005% alizarin red in 0.9 N acetic acid and 60% ethanol overnight at room temperature and

cleared with 1% KOH for overnight followed by 20% glycerol in 1% KOH until cleared.

For whole mount in situ hybridization, embryos were dissected from pregnant mice, fixed overnight in 4% PFA at 4 °C. The fixed embryos were dehydrated through 25%, 50%, 75%, and 100% ethanol, and stored in 100% ethanol at −20 °C. Whole mount in situ hybridization was carried out using previously described protocol (Belo et al., 1997) with hybridization temperature of 65 °C.

Palatal shelf organ culture

Palatal shelves were cultured according to previously described methods (Brunet et al., 1995; Taya et al., 1999). Palatal shelves were removed at E13.5 from wild type and *Wnt1-Cre;Nog*^*lacz/fx* embryos. Paired palatal shelves were placed on 0.3 μm Millipore filters with medial edge epithelia (MEE) in contact. Initially, paired palatal shelves were cultured in Minimal Essential Medium with Earle's salts and L-glutamine (Gibco) supplemented with 1% anti-anti (Gibco) at 37 °C in a 5% CO_2 air environment. After 24 h culture the paired palatal shelves were submerged in DMEM with Earle's salts and L-glutamine (Gibco) supplemented with 5% FBS for another 48 h. After total 72 h of culture, paired palatal shelves were fixed in 4% PFA and processed for paraffin blocks and sectioned at a 10-μm thickness as described above.

Quantitative real-time reverse transcription-polymerase chain reaction (q-PCR)

RNA was purified from E12.5 and E13.5 palatal tissue or mandibles from wild type and mutant samples using Trizol reagents (Invitrogen). Following RNA extraction, cDNA was synthesized using iScript™ cDNA Synthesis Kit (BIO RAD). Quantitative PCR amplifications were performed in a StepOnePlus real-time PCR machine (Applied Biosystems) using the SensiMix™ SYBR & Fluorescein Kit (Bioline). For each gene, the PCR reaction was carried out in triplicates and the relative levels of mRNAs were normalized to that of HPRT using the normalized expression method. Student's *t*-test was used to analyze the significance of difference and a *P*-value less than 0.05 was considered statistically significant.

Detection of cell proliferation

For detection of cell proliferation in the palatal shelves, pregnant female mice were injected once intraperitoneally at gestational day 12.5 and 13.5 with BrdU Labeling Reagent (50 μg/g body weight; Roche). 30 min after injection, embryos were dissected, fixed with 4% PFA overnight at 4 °C and embedded in paraffin for 10 μm-thickness coronal sectioning. To detect BrdU, rat anti-BrdU (1:500; Accurate Chemical & Scientific) and Alexa Fluor-conjugated secondary antibody (1:500; Invitrogen) were used. Following BrdU immunostaining, cell counts were recorded for each of the bilateral palatal shelves of matching areas of anterior secondary palate and of posterior secondary palate regions in the wild type and mutant samples. The cell proliferation rate was calculated as the number of the cell nuclei with BrdU labeling. Alternatively, mouse anti-phosphorylated histone H3 (1:500; cell signaling) and Alexa Fluor-conjugated secondary antibody (1:500; Invitrogen) were also used to detect dividing cells. Data were collected from at least three pairs of mutant and wild type littermates at each developmental stage. Students' *t*-test was used to analyze the significance of difference and a *P*-value less than 0.05 was considered statistically significant.

Appendix A. Supplementary materials

Supplementary data associated with this article can be found in the online version at http://dx.doi.org/10.1016/j.ydbio.2014.06.006.

References

Anderson, R.M., Lawrence, A.R., Stottmann, R.W., Bachiller, D., Klingensmith, J., 2002. Chordin and Noggin promote organizing centers of forebrain development in the mouse. Development 129, 4975–4987.

Anderson, R.M., Stottmann, R.W., Choi, M., Klingensmith, J., 2006. Endogenous bone morphogenetic protein antagonists regulate mammalian neural crest generation and survival. Dev. Dyn. 235, 2507–2520.

Bachiller, D., Klingensmith, J., Kemp, C., Belo, J.A., Anderson, R.M., May, S.R., McMahon, J.A., McMahon, A.P., Harland, R.M., Rossant, J., De Robertis, E.M., 2000. The organizer factors Chordin and Noggin are required for mouse forebrain development. Nature 403, 658–661.

Baek, J.A., Lan, Y., Liu, H., Maltby, K.M., Mishina, Y., Jiang, R.L., 2011. Bmpr1a signaling plays critical roles in palatal shelf growth and palatal bone formation. Dev. Biol. 350, 520–531.

Belo, J.A., Bouwmeester, T., Leyns, L., Kertesz, N., Gallo, M., Follettie, M., De Robertis, E.M., 1997. Cerberus-like is a secreted factor with neutralizing activity expressed in the anterior primitive endoderm of the mouse gastrula. Mech. Dev. 68, 45–57.

Bonilla-Claudio, M., Wang, J., Bai, Y., Klysik, E., Selever, J., Martin, J.F., 2012. Bmp signaling regulates a dose-dependent transcriptional program to control facial skeletal development. Development 139, 709–719.

Braybrook, C., Doudney, K., Marcano, A.C., Arnason, A., Bjornsson, A., Patton, M.A., Goodfellow, P.J., Moore, G.E., Stanier, P., 2001. The T-box transcription factor gene TBX22 is mutated in X-linked cleft palate and ankyloglossia. Nat. Genet. 29, 179–183.

Brewer, S., Feng, W., Huang, J., Sullivan, S., Williams, T., 2004. Wnt1-Cre-mediated deletion of AP-2alpha causes multiple neural crest-related defects. Dev. Biol. 267, 135–152.

Brunet, C.L., Sharpe, P.M., Ferguson, M.W., 1995. Inhibition of TGF-beta 3 (but not TGF-beta 1 or TGF-beta 2) activity prevents normal mouse embryonic palate fusion. Int. J. Dev. Biol. 39, 345–355.

Brunet, L.J., McMahon, J.A., McMahon, A.P., Harland, R.M., 1998. Noggin, cartilage morphogenesis, and joint formation in the mammalian skeleton. Science 280, 1455–1457.

Burstyn-Cohen, T., Kalcheim, C., 2002. Association between the cell cycle and neural crest delamination through specific regulation of G1/S transition. Dev. Cell. 3, 383–395.

Chai, Y., Jiang, X., Ito, Y., Bringas Jr., P., Han, J., Rowitch, D.H., Soriano, P., McMahon, A. P., Sucov, H.M., 2000a. Fate of the mammalian cranial neural crest during tooth and mandibular morphogenesis. Development 127, 1671–1679.

Chai, Y., Jiang, X.B., Ito, Y., Bringas, P., Han, J., Rowitch, D.H., Soriano, P., McMahon, A. P., Sucov, H.M., 2000b. Fate of the mammalian cranial neural crest during tooth and mandibular morphogenesis. Development 127, 1671–1679.

Choi, M., Klingensmith, J., 2009. Chordin is a modifier of tbx1 for the craniofacial malformations of 22q11 deletion syndrome phenotypes in mouse. PLoS Genet. 5, e1000395.

Couly, G., Creuzet, S., Bennaceur, S., Vincent, C., Le Douarin, N.M., 2002. Interactions between Hox-negative cephalic neural crest cells and the foregut endoderm in patterning the facial skeleton in the vertebrate head. Development 129, 1061–1073.

d'Amaro, R., Scheidegger, R., Blumer, S., Pazera, P., Katsaros, C., Graf, D., Chiquet, M., 2012. Putative functions of extracellular matrix glycoproteins in secondary palate morphogenesis. Front. Physiol. 3, 377.

Danielian, P.S., Muccino, D., Rowitch, D.H., Michael, S.K., McMahon, A.P., 1998. Modification of gene activity in mouse embryos in utero by a tamoxifen-inducible form of Cre recombinase. Curr. Biol. 8, 1323–1326.

Dudas, M., Sridurongrit, S., Nagy, A., Okazaki, K., Kaartinen, V., 2004. Craniofacial defects in mice lacking BMP type I receptor Alk2 in neural crest cells. Mech. Dev. 121, 173–182.

Fuchs, A., Inthal, A., Herrmann, D., Cheng, S., Nakatomi, M., Peters, H., Neubuser, A., 2010. Regulation of Tbx22 during facial and palatal development. Dev. Dyn. 239, 2860–2874.

Gato, A., Martinez, M.L., Tudela, C., Alonso, I., Moro, J.A., Formoso, M.A., Ferguson, M. W., Martinez-Alvarez, C., 2002. TGF-beta(3)-induced chondroitin sulphate proteoglycan mediates palatal shelf adhesion. Dev. Biol. 250, 393–405.

Goldstein, A.M., Brewer, K.C., Doyle, A.M., Nagy, N., Roberts, D.J., 2005. BMP signaling is necessary for neural crest cell migration and ganglion formation in the enteric nervous system. Mech. Dev. 122, 821–833.

Goodrich, L.V., Milenkovic, L., Higgins, K.M., Scott, M.P., 1997. Altered neural cell fates and medulloblastoma in mouse patched mutants. Science 277, 1109–1113.

Hall, R.J., Erickson, C.A., 2003. ADAM 10: an active metalloprotease expressed during avian epithelial morphogenesis. Dev. Biol. 256, 146–159.

Harfe, B.D., Scherz, P.J., Nissim, S., Tian, H., McMahon, A.P., Tabin, C.J., 2004. Evidence for an expansion-based temporal Shh gradient in specifying verte-brate digit identities. Cell. 118, 517–528.

He, F., Xiong, W., Wang, Y., Matsui, M., Yu, X., Chai, Y., Klingensmith, J., Chen, Y., 2010. Modulation of BMP signaling by Noggin is required for the maintenance of palatal epithelial integrity during palatogenesis. Dev. Biol. 347, 109–121.

Higashihori, N., Buchtova, M., Richman, J.M., 2010. The function and regulation of TBX22 in avian frontonasal morphogenesis. Dev. Dyn. 239, 458–473.

Holder-Espinasse, M., Abadie, V., Cormier-Daire, V., Beyler, C., Manach, Y., Munnich, A., Lyonnet, S., Couly, G., Amiel, J., 2001. Pierre Robin sequence: a series of 117 consecutive cases. J. Pediatrics 139, 588–590.

Hu, D., Colnot, C., Marcucio, R.S., 2008. Effect of bone morphogenetic protein signaling on development of the jaw skeleton. Dev. Dyn. 237, 3727–3737.

Huang, X., Yokota, T., Iwata, J., Chai, Y., 2011. Tgf-beta-mediated FasL-Fas-Caspase pathway is crucial during palatogenesis. J. Dent. Res. 90, 981–987.

Jeong, J., Mao, J., Tenzen, T., Kottmann, A.H., McMahon, A.P., 2004. Hedgehog signaling in the neural crest cells regulates the patterning and growth of facial primordia. Genes Dev. 18, 937–951.

Jiang, X., Rowitch, D.H., Soriano, P., McMahon, A.P., Sucov, H.M., 2000. Fate of the mammalian cardiac neural crest. Development 127, 1607–1616.

Kanzler, B., Foreman, R.K., Labosky, P.A., Mallo, M., 2000. BMP signaling is essential for development of skeletogenic and neurogenic cranial neural crest. Develop-ment 127, 1095–1104.

Klingensmith, J., Matsui, M., Yang, Y.P., Anderson, R.M., 2010. Roles of bone morphogenetic protein signaling and its antagonism in holoprosencephaly. Am. J. Med. Genet. Part C Semin. Med. Genet. 154C, 43–51.

Lana-Elola, E., Tylzanowski, P., Takatalo, M., Alakurtti, K., Veistinen, L., Mitsiadis, T. A., Graf, D., Rice, R., Luyten, F.P., Rice, D.P., 2011. Noggin null allele mice exhibit a microform of holoprosencephaly. Hum. Mol. Genet. 20, 4005–4015.

Li, L., Wang, Y., Lin, M., Yuan, G., Yang, G., Zheng, Y., Chen, Y., 2013. Augmented BMPRIA-mediated BMP signaling in cranial neural crest lineage leads to cleft palate formation and delayed tooth differentiation. PloS One 8, e66107.

Matsui, M., Klingensmith, J., 2013. Development of the Craniofacial Skeleton, Primer on the Metabolic Bone Diseases and Disorders of Mineral Metabolism. John Wiley & Sons, Inc., pp. 893–903.

McBratney-Owen, B., Iseki, S., Bamforth, S.D., Olsen, B.R., Morriss-Kay, G.M., 2008. Development and tissue origins of the mammalian cranial base. Dev. Biol. 322, 121–132.

McMahon, J.A., Takada, S., Zimmerman, L.B., Fan, C.M., Harland, R.M., McMahon, A. P., 1998. Noggin-mediated antagonism of BMP signaling is required for growth and patterning of the neural tube and somite. Genes Dev. 12, 1438–1452.

Melnick, M., Witcher, D., Bringas Jr., P., Carlsson, P., Jaskoll, T., 2005. Meckel's cartilage differentiation is dependent on hedgehog signaling. Cells Tissues Organs 179, 146–157.

Minina, E., Kreschel, C., Naski, M.C., Ornitz, D.M., Vortkamp, A., 2002. Interaction of FGF, Ihh/Pthlh, and BMP signaling integrates chondrocyte proliferation and hypertrophic differentiation. Dev. Cell. 3, 439–449.

Minina, E., Wenzel, H.M., Kreschel, C., Karp, S., Gaffield, W., McMahon, A.P., Vortkamp, A., 2001. BMP and Ihh/PTHrP signaling interact to coordinate chondrocyte proliferation and differentiation. Development 128, 4523–4534.

Molsted, K., Dahl, E., Skovgaard, L.T., Asher-McDade, C., Brattstrom, V., McCance, A., Prahl-Andersen, B., Semb, G., Shaw, B., The, R., 1993. A multicentre comparison of treatment regimens for unilateral cleft lip and palate using a multiple regression model. Scand. J. Plast. Reconstruct. Surg. Hand Surg./Nord. Plastik-kirurgisk forening [and] Nord. Klubb Handkirurgi 27, 277–284.

Molsted, K., Kjaer, I., Dahl, E., 1995. Cranial base in newborns with complete cleft lip and palate: radiographic study. Cleft Palate Craniofac. J. 32, 199–205.

Morris-Wiman, J., Brinkley, L., 1992. An extracellular matrix infrastructure provides support for murine secondary palatal shelf remodelling. Anat. Rec. 234, 575–586.

Mossey PA, L.J., 2002. Epidemiology of Oral Cleft: An Internationa Perspective. Oxford University Press, New York, NY.

Nawshad, A., Medici, D., Liu, C.C., Hay, E.D., 2007. TGFbeta3 inhibits E-cadherin gene expression in palate medial-edge epithelial cells through a Smad2-Smad4-LEF1 transcription complex. J. Cell Sci. 120, 1646–1653.

Nifuji, A., Noda, M., 1999. Coordinated expression of noggin and bone morphoge-netic proteins (BMPs) during early skeletogenesis and induction of noggin expression by BMP-7. J. Bone Miner. Res. 14, 2057–2066.

Pauws, E., Moore, G.E., Stanier, P., 2009. A functional haplotype variant in the TBX22 promoter is associated with cleft palate and ankyloglossia. J. Med. Genet. 46, 555–561.

Potti, T.A., Petty, E.M., Lesperance, M.M., 2011. A comprehensive review of reported heritable noggin-associated syndromes and proposed clinical utility of one broadly inclusive diagnostic term: NOG-related-symphalangism spectrum dis-order (NOG-SSD). Hum. Mutat. 32, 877–886.

Pruzinsky, T., 1992. Social and psychological effects of major craniofacial deformity. Cleft Palate Craniofac. J. 29, 578–584 (discussion 570).

Rodriguez, P., Da Silva, S., Oxburgh, L., Wang, F., Hogan, B.L., Que, J., 2010. BMP signaling in the development of the mouse esophagus and forestomach. Development 137, 4171–4176.

St-Jacques, B., Hammerschmidt, M., McMahon, A.P., 1999. Indian hedgehog signal-ing regulates proliferation and differentiation of chondrocytes and is essential for bone formation. Genes Dev. 13, 2072–2086.

Stafford, D.A., Brunet, L.J., Khokha, M.K., Economides, A.N., Harland, R.M., 2011. Cooperative activity of noggin and gremlin 1 in axial skeleton development. Development 138, 1005–1014.

Stottmann, R.W., Anderson, R.M., Klingensmith, J., 2001. The BMP antagonists Chordin and Noggin have essential but redundant roles in mouse mandibular outgrowth. Dev. Biol. 240, 457–473.

Stottmann, R.W., Klingensmith, J., 2011. Bone morphogenetic protein signaling is required in the dorsal neural folds before neurulation for the induction of spinal neural crest cells and dorsal neurons. Dev. Dyn. 240, 755–765.

Taya, Y., O'Kane, S., Ferguson, M.W., 1999. Pathogenesis of cleft palate in TGF-beta3 knockout mice. Development 126, 3869–3879.

Wang, Y., Zheng, Y., Chen, D., Chen, Y., 2013. Enhanced BMP signaling prevents degeneration and leads to endochondral ossification of Meckel's cartilage in mice. Dev. Biol. 381, 301–311.

Warren, S.M., Brunet, L.J., Harland, R.M., Economides, A.N., Longaker, M.T., 2003. The BMP antagonist noggin regulates cranial suture fusion. Nature 422, 625–629.

Xu, X., Han, J., Ito, Y., Bringas Jr., P., Urata, M.M., Chai, Y., 2006. Cell autonomous requirement for Tgfbr2 in the disappearance of medial edge epithelium during palatal fusion. Dev. Biol. 297, 238–248.

Yu, L., Gu, S., Alappat, S., Song, Y., Yan, M., Zhang, X., Zhang, G., Jiang, Y., Zhang, Z., Zhang, Y., Chen, Y., 2005. Shox2-deficient mice exhibit a rare type of incomplete clefting of the secondary palate. Development 132, 4397–4406.